



Cite this: *RSC Adv.*, 2017, 7, 33241

# Persistent photocatalysis effect of black peony-like BiOCl and its potential full-time photocatalytic applications†

Pengfei Feng,<sup>‡a</sup> Xue Tang,<sup>‡a</sup> Jiachi Zhang,<sup>‡a</sup> Yuehai Mei<sup>a</sup> and Huihui Li<sup>\*a</sup>

A new concept of a "Persistent Photocatalysis (PersP)" effect is defined for the first time according to the observation that the black peony-like BiOCl material is able to efficiently degrade Rhodamine B dye after removing visible light irradiation, just as in persistent luminescence of phosphors. The discovery of the PersP effect provides a potential solution to realize full-time photocatalytic applications. The PersP effect was justified through a series of decomposition experiments, and its potential prospect for full-time application was evaluated by experiments as well. On the basis of the results, a possible PersP mechanism of the black peony-like BiOCl material has been proposed.

Received 8th May 2017  
 Accepted 22nd June 2017

DOI: 10.1039/c7ra05185a

[rsc.li/rsc-advances](http://rsc.li/rsc-advances)

## Introduction

In recent years, researchers have focused on semiconductor photocatalysis due to its potential applications in energy conversion and degradation of environmental pollutants.<sup>1–4</sup> The reported photocatalyst systems, to the best of our knowledge, can be generally classified as oxides,<sup>5–7</sup> sulfides,<sup>8,9</sup> oxysulfides,<sup>10</sup> nitrides<sup>11</sup> and oxynitrides.<sup>12</sup> However, all the present photocatalysts can only be promoted under ultraviolet or visible light irradiation and thus do not work when the light source is not present (for example at night). In addition, it is very difficult to treat the pollutants in dark conditions such as non-transparent or low-transparency wastewater, due to the limited light penetration.

In order to realize the full-time photocatalytic applications, H. H. Li and P. F. Feng had previously used the persistent luminescence (PersL) of phosphor to support the photocatalytic activity in dark conditions.<sup>13–16</sup> However, the persistent luminescence is actually weak and can be badly quenched in water. Additionally, the energy transfer by light absorption (phosphor → photocatalyst) is inefficient. Consequently, the present PersL assistant photocatalysts are not valuable for the practical full-time photocatalytic applications.<sup>13–16</sup> Therefore, there is an urgent desire to develop a new photocatalyst which is able to

exhibit the photocatalytic activity even after removing irradiation light source.

Essentially, the photocatalysis is involved in a photo-induced process: under light irradiation, some photo-generated carriers (electrons and holes) are created and then they are involved in the subsequent oxidation–reduction reactions *i.e.*, photocatalysis. However, if the photo-created carriers can be captured and stored in some shallow traps and then are thermally released in low speed after removing the irradiation light source, it may show the "delayed" persistent photocatalysis (PersP) effect, just like the "delayed" persistent luminescence (PersL). Significantly, this PersP effect may be used in potential full-time applications.

According to some references on PersL, the traps with appropriate depths are very significant for the PersL properties of phosphors, and the traps in most efficient PersL phosphors are highly associated with the intrinsic oxygen vacancies ( $V_o^{\cdot}$ ).<sup>17–22</sup> On the other hand, according to some references on photocatalysis, the oxygen vacancies can be generally induced in BiOCl by reduction method using Fe,<sup>23</sup> nitrogen doping<sup>24</sup> or UV light irradiation.<sup>3,25</sup> The BiOCl photocatalyst with rich oxygen vacancies shows black body, and it exhibits high photocatalytic ability under visible light irradiation.<sup>3,23,25–27</sup> Accordingly, although the delayed photocatalysis effect can be expected in the black BiOCl materials due to the presence of lots of oxygen vacancies, however, the PersP effect has been never reported thus far. Moreover, it must be strongly stressed that although L. Li has reported that the PersL and photocatalytic behaviours of the ZnGa<sub>2</sub>O<sub>4</sub> materials, obviously, Li's observation is completely unrelated to the PersP concept newly proposed in this paper.<sup>28</sup>

In this work, we have synthesized a black peony-like BiOCl material, and we have successfully observed the persistent photocatalysis (PersP) effect after removing the visible irradiation light, just like the PersL behaviour of phosphor. The PersP effect and the potential prospect of full-time applications have

<sup>a</sup>Key Laboratory for Magnetism Magnetic Materials of the Ministry of Education, Lanzhou University, Lanzhou 730000, P. R. China. E-mail: zhangjch@lzu.edu.cn; lihh@lzu.edu.cn; Fax: +86-931-8913554; Tel: +86-931-8912772

<sup>b</sup>Key Laboratory of Special Function Materials and Structure Design, Ministry of Education, Lanzhou University, Lanzhou 730000, P. R. China

† Electronic supplementary information (ESI) available. See DOI: 10.1039/c7ra05185a

‡ These authors contributed equally to this work.



been justified through a serial of decomposition experiments in solution. According to these results, a possible PersP mechanism of the black peony-like nano BiOCl material has been proposed.

## Experimental

### Materials and synthesis

All chemical reagents used in the experiments were analytical grade and received without further purification. Briefly, 0.03 g Bi<sub>2</sub>O<sub>3</sub> powder was dissolved in an excess of concentrated hydrochloric acid to receive a transparent BiCl<sub>3</sub>-HCl aqueous solution. Subsequently, 0.01 g polyvinylpyrrolidone (PVP) were dissolved in the solution. Then, the peony-like BiOCl samples were generated when the water was added, and the ultrasonic treatment and mechanical agitation lasted for 30 min. The final products with write body were washed with anhydrous ethanol several times and dried in air at 60 °C for 2 h before various characterizations. And then, the white peony-like BiOCl samples were subjected to irradiation using an ultraviolet lamp (500 W high-pressure mercury lamp) for 5 h with H<sub>2</sub> blowing, and the final black peony-like BiOCl sample was obtained.

### Photocatalytic experiments

The photocatalytic activities of samples were tested by the decomposition of RhB in solution ( $m_{\text{BiOCl}} = 20 \text{ mg}$ ,  $C_0 = 20 \text{ mg L}^{-1}$ ,  $V = 50 \text{ mL}$ ). Long-wavelength pass filter ( $\lambda \geq 420 \text{ nm}$ ) was equipped with a 500 W xenon lamp to get visible light. In a typical PersP test, the sample (20 mg) was firstly irradiated by the visible light ( $\lambda \geq 420 \text{ nm}$ ) for 5 h and then the sample was individually suspended in the RhB solution (20 mg L<sup>-1</sup>, 50 mL) in a completely dark room. A certain volume of the suspension was withdrawn at selected times for analysis. The full-time photocatalytic test is carried out in sunlight environment: 20 mg black peony-like BiOCl sample (without previous irradiation) and 50 mL RhB solution (20 mg L<sup>-1</sup>) were added in a quartz beaker and covered with plastic film. Then, the beaker was irradiated with a sunlight simulator (AM 1.5G) and the solution was withdrawn at selected times for analysis.

### Measurements and characterization

The crystal phases of the obtained materials were determined by a Rigaku (Tokyo, Japan) D/Max-2400 X-ray diffractometer (XRD) using CuK<sub>α</sub> irradiation ( $k = 1.5406 \text{ \AA}$ ) with a scanning step 0.02° over the 2θ range from 10° to 80°, the acquisition time for each step is 0.1 s. The morphology of samples was inspected with the scanning electron microscopy (SEM, Thermo, USA, S-4800). A FEI Tecnai G2 F30 transmission electron microscope (FEI, Hillsboro, OR) equipped with a Gatan imaging filter (GIF) system was used for transmission electron microscopy (TEM), high-resolution transmission electron microscopy (HRTEM), selected-area electron-diffraction pattern (SAED) and Energy Dispersive X-ray spectroscopy (EDX). The TEM samples were prepared as follows: approximately 1–2 mg powder was dispersed in anhydrous alcohol for 30 min to form a suspension. A few drops of this suspension were dripped onto formvar

stabilized with carbon support films and were dried for several hours. The concentration of the RhB solution was analysed by measuring the light absorption of the clear solution using a UV-vis spectrophotometer (Analytic Jena AG, Specord 50). The percentage of degradation was calculated as  $C/C_0$ , where  $C$  is the concentration of the remaining dye solution and  $C_0$  is the initial concentration. Measurements of full-time photocatalytic applications were performed with a sunlight simulator (Keithley-2400, Tektronix, Beaverton, USA).

## Results and discussion

The X-ray diffraction (XRD) patterns of the white (blue line) and black (red line) peony-like BiOCl samples were shown in Fig. 1, respectively. These patterns are all in good accordance with the standard card (PDF#85-0861). There are no other impurity XRD peaks observed in the patterns. In addition, the intense peaks represent the well crystallized prepared products. It can be seen that the (102) facets are stronger than any other peaks in samples. The difference from the standard card may be attributed to the different crystal panel direction under various preparation conditions. The inset of Fig. 1 gives the energy dispersive X-ray spectroscopy (EDX) spectra of the both samples, and it indicates that, apart from traces of Cu and C resulting from the transmission electron microscopy (TEM) grid, only Bi, Cl and O elements are present. The results demonstrate that the as-prepared white and black peony-like samples are BiOCl.

Fig. 2a and c shows the SEM images of the as-synthesized white BiOCl sample. It is clearly observed that the special peony-like architectures are based on 2D nano-plates. The surface of the nano-plates is flat and the maximum thickness does not exceed 100 nm. The SEM images of the black BiOCl are also shown in Fig. 2b and d. It can be seen that the irradiation does not change the peony-like structure of BiOCl particles. It is known to all that the BiOCl materials with different exposed

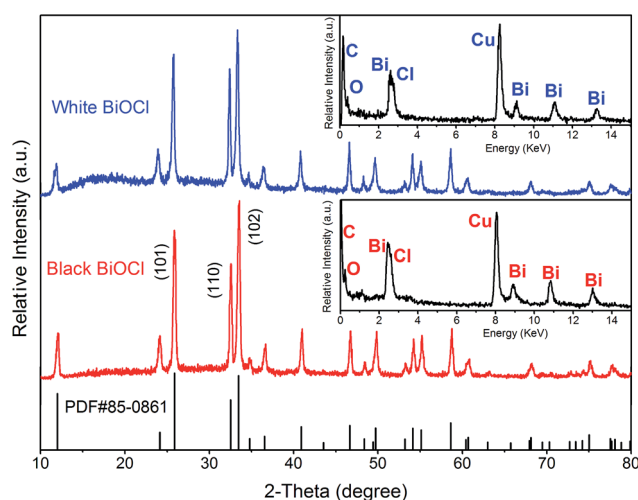


Fig. 1 The X-ray diffraction (XRD) patterns of the white (blue line) and black (red line) peony-like BiOCl samples, the insert, the energy dispersive X-ray spectroscopy (EDX) spectra of the samples.



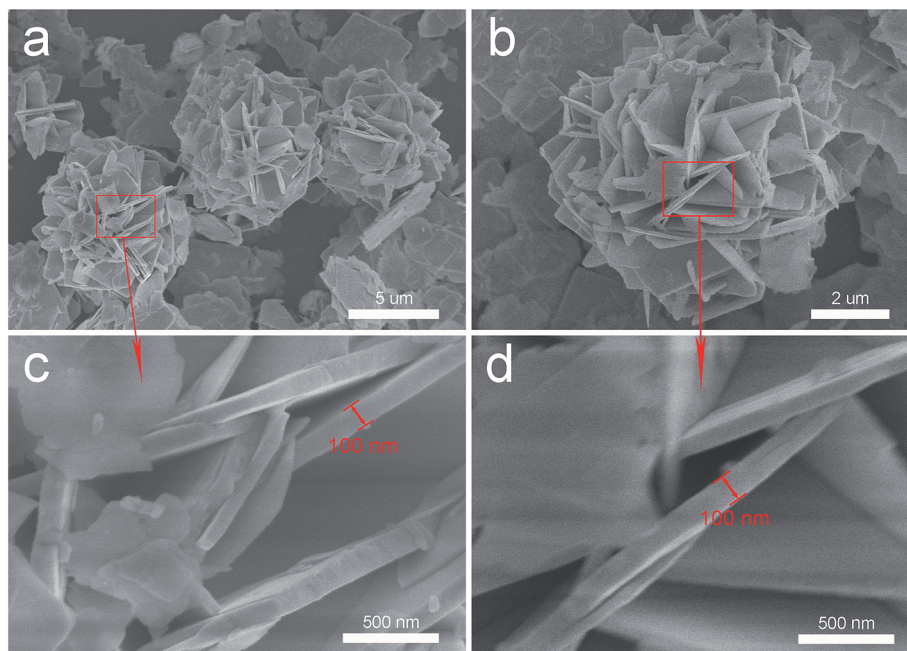


Fig. 2 The SEM images of the white (a, c) and black (b, d) peony-like BiOCl samples.

planes generally show different photocatalytic properties and the exposed {001} facets exhibit much higher activity for pollutant degradation.<sup>27,29,30</sup> In order to explore the exposed facets for each petal in BiOCl peony, we analysed the samples by

transmission electron microscope (TEM). At first, the TEM images of the white (a) and black (e) BiOCl samples further confirm the peony-like shape of the particles. The high-resolution (HRTEM) image of the black peony-like BiOCl

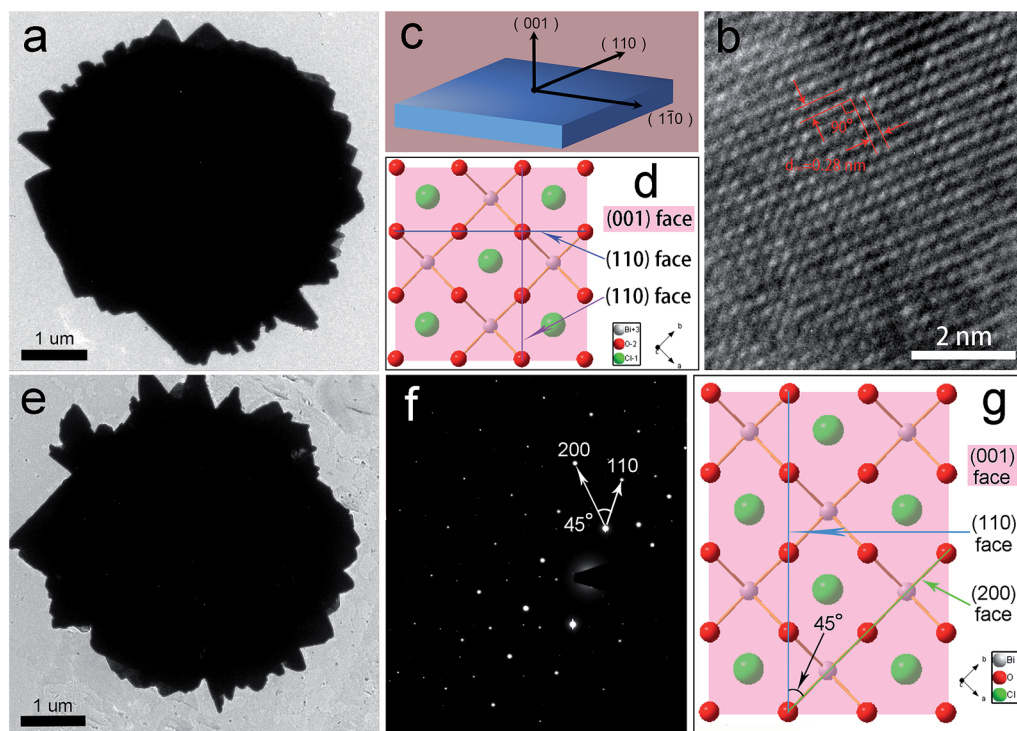


Fig. 3 The TEM images of the white (a) and black (e) BiOCl samples; (b) the high-resolution (HRTEM) image of the black peony-like BiOCl sample; (c) the relationship between the (1-10) (110) and (001) faces; (d) atomic structure of the {001} facets; (f) the selected area electron diffraction SAED pattern of the single-crystalline in the black BiOCl peony; (g) the relationship between the (110) and (200) planes.



sample is shown in Fig. 3b. The clear lattice fringes with interplanar lattice spacing of 0.28 nm correspond to the (110) atomic planes of the square crystal phase of BiOCl. The bottom and top surfaces of the petal in BiOCl peony are identified as {001} facets,<sup>25</sup> while the four lateral surfaces are {110} facets (Fig. 3c). The atomic structure of the {001} facets is characterized by the high density of oxygen atoms (Fig. 3d).<sup>30</sup> In addition, the selected area electron diffraction SAED pattern (Fig. 3f) indicates the single-crystalline characteristic of the petal in the black BiOCl peony. The angle labeled in the SAED pattern is 45°, which is in agreement with the theoretical value of the angle between the (110) and (200) planes (as show in Fig. 3g). The diffraction spots can be indexed as [001] zone axis of tetragonal BiOCl.<sup>30</sup>

Fig. 4a shows the UV-Vis reflection spectra of the white (blue line) and black (red line) peony-like BiOCl samples and the commercial TiO<sub>2</sub> (P25) samples (black line). It can be observed that the white BiOCl sample does not show any absorption in the visible range. On the contrary, the black BiOCl sample exhibits obvious absorption in a very broad range, and thus it imply a full-spectral response due to the presence of lots of the oxygen vacancies.<sup>3,23,25,27</sup>

Fig. 4 depicts the computed band structures of the white (c) and black (d) BiOCl samples, respectively. The densities of states (DOS) are shown in Fig. 4b. The band gap has been corrected by a scissor value (3.44 eV) based on the diffuse reflectance spectrum of the pure BiOCl (white BiOCl) as shown in the insert of Fig. 4b. It can be seen in Fig. 4c that the valence band

maximum (VBM) is located on the *k*-point line of Z–R, while the conduction band minimum (CBM) is located at the *k*-point of Z, which means BiOCl is an indirect band gap semiconductor. On the other hand, as shown in Fig. 4d, for the black BiOCl sample, a new impurity level (red line) stems from the oxygen vacancies (V<sub>o</sub><sup>••</sup>) can be observed and it is located just below the CBM ( $\Delta E = 1.07$  eV). The densities of states (DOS) of the V<sub>o</sub><sup>••</sup> is also shown in Fig. 4b. Although the level of the V<sub>o</sub><sup>••</sup> looks like a single line in the computed band gap, it actually should be a broad band. As a consequence, the black BiOCl with presence of lots of V<sub>o</sub><sup>••</sup> can absorb visible light. On the other hand, it is important to note that the computed level of the V<sub>o</sub><sup>••</sup> is only 1.07 eV lower than the CBM. It means that the photo-induced electrons can be captured and stored in oxygen vacancies as traps for an appropriately long time and then the captured electrons can be thermally released to induce the “delayed” oxidation–reduction reactions at room temperature due to the appropriate depth of the traps, just like delayed luminescence (*i.e.*, persistent luminescence). Therefore, at this stage, a “delayed” persistent photocatalysis effect can be expected in this black peony-like BiOCl sample in theory, and accordingly this new effect can be named as “persistent photocatalysis (PersP)” effect.

The photocatalytic ability of the black peony-like BiOCl sample under ultraviolet or visible irradiation has been evaluated by other groups,<sup>3,17,19–21</sup> and our experiments give the similar results as shown in Fig. 5 and S1.† In this work, we mainly focus on the newly discovered PersP effect and the potential full-time applications of the black peony-like BiOCl

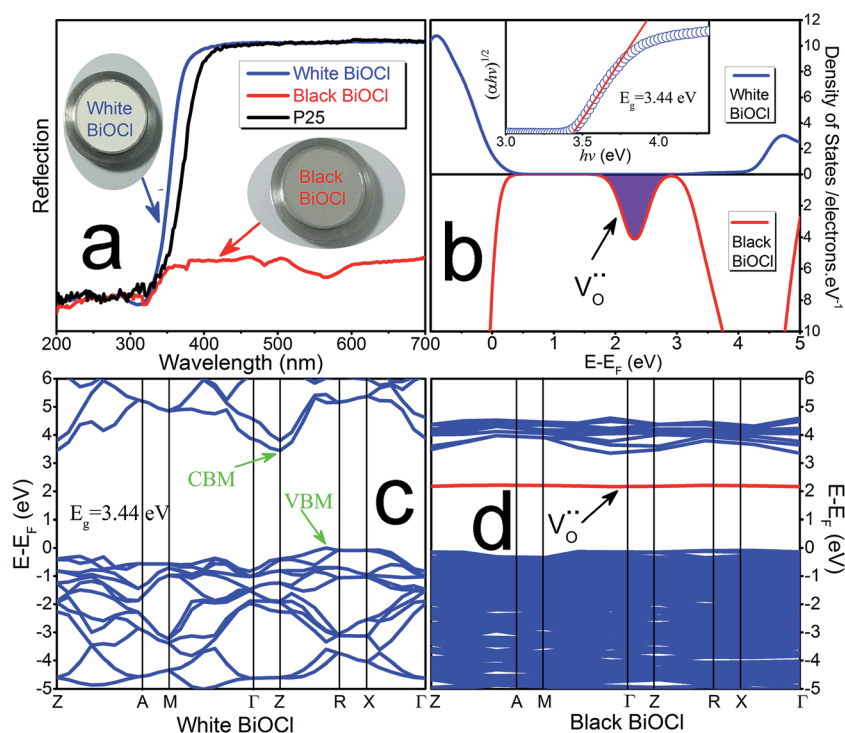


Fig. 4 The UV-Vis reflection spectra of the white (blue line) and black (red line) peony-like BiOCl samples and the commercial TiO<sub>2</sub> samples (black line) (a) the densities of states (DOS) of the white (up) and black (down) BiOCl samples (b) band structures of the white (c) and black (d) BiOCl samples. The insert,  $(\alpha hv)^{1/2}$  variation versus photon energy  $h\nu$ .



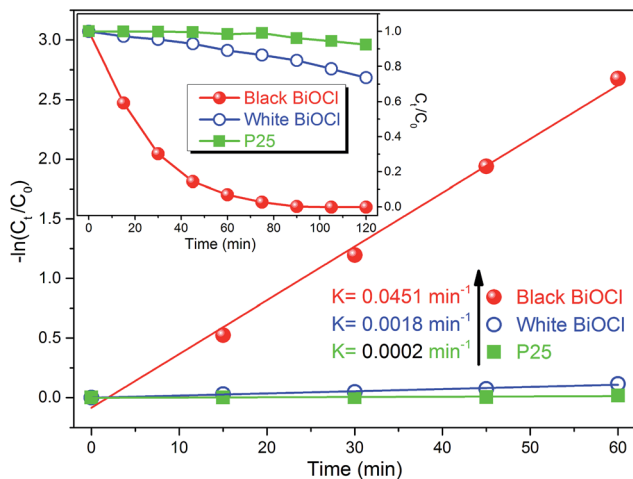


Fig. 5 The photocatalytic ability of the white and black peony-like BiOCl samples and the commercial TiO<sub>2</sub> samples under visible irradiation.

samples. In order to justify the PersP effect, 20 mg TiO<sub>2</sub> (P25) (green line), white (blue line) and black (red line) peony-like BiOCl samples were firstly irradiated by a visible light source (500 W xenon lamp,  $\lambda \geq 420 \text{ nm}$ ) for 5 h and then were put into the RhB solutions (20 mg L<sup>-1</sup>, 50 mL) in a completely dark room. For the references, the parallel experiments without visible light irradiation had been conducted as well. The

original UV/Vis spectra of the RhB solutions at different time are also given in Fig. S2.† As shown in Fig. 6a, it is found that only the black peony-like BiOCl sample after visible light irradiation shows obvious decomposition of RhB dye and the RhB could be degraded completely in 8 h in the darkness. The TOC experiment also confirms that this is a process of degradation and is not an adsorption or mineralization process, as shown in Fig. S3.† On the contrary, the other samples only show slight reduction (<20%) due to the physical adsorption and desorption of RhB or weak degradation. Comparing the RhB degradation curve effected by the irradiated black BiOCl and un-irradiated black BiOCl samples, we can confirm that the obtained black peony-like BiOCl sample shows obvious PersP effect (as show in Fig. S4,† the shadow part can be recognized as the PersP effect) and it of course can be used in potential full-time photocatalytic applications. Perhaps the most interestingly, it is found that the PersP decomposition curve decreases quickly at first and then very slowly, which is just like the decay curve of the PersL. Moreover, the decomposition curve cannot be fitted well by a straight line ( $R^2 = 98.29\%$ ) in the diagram of  $-\ln(C/C_0)$  vs.  $t$  as shown in Fig. 6b, indicating that the PersP process is not a first order reaction. But, it can be fitted very well by a second order decay function as shown in Fig. 6c, which is usually used to analyse PersL properties of phosphor. This result indicates that the mechanism of PersP effect should be highly associated with the thermal release of electrons in traps ( $V_{\text{O}}^{\bullet}$ ) just like PersL.<sup>20,22,31–33</sup> Cycled runs of the PersP experiments have been

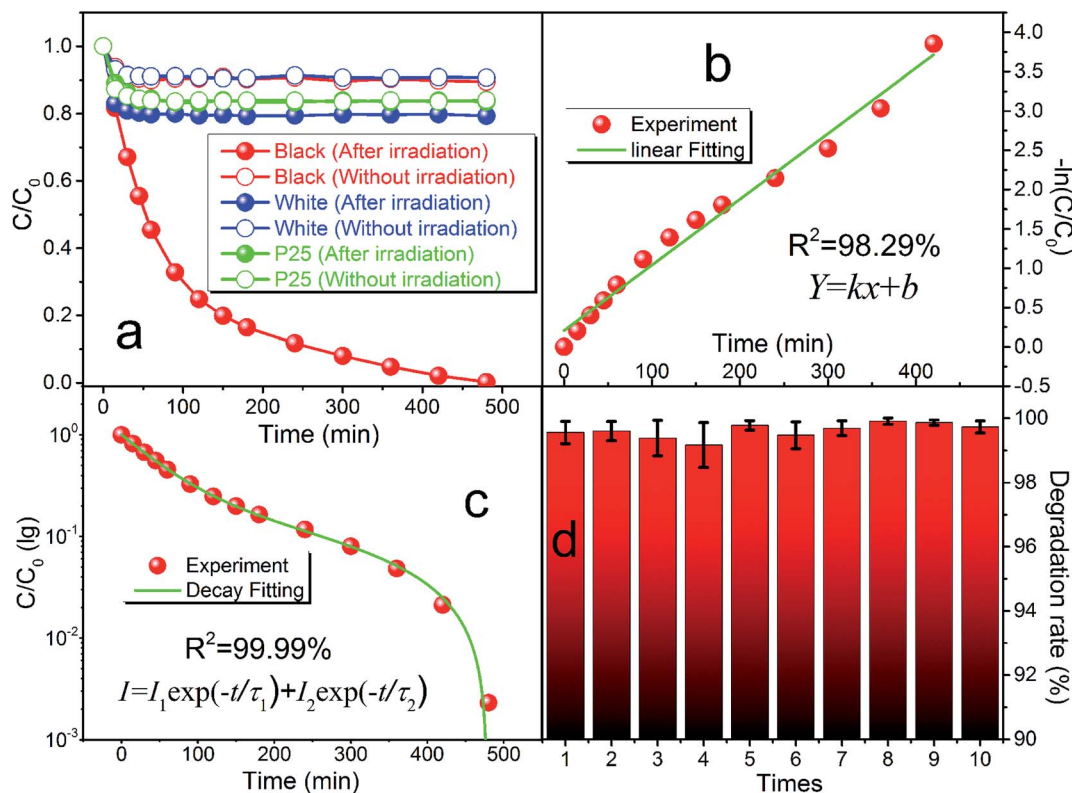


Fig. 6 (a) The PersP effect of these samples. (b) The liner fitting of the decomposition curve of the black peony-like BiOCl sample after irradiation. (c) The decay fitting of the black peony-like BiOCl sample after irradiation. (d) The PersP stability of the black peony-like BiOCl.



also tested using the black peony-like BiOCl sample after visible light irradiation. The PersP ability doesn't show a decline even after 10 cycles as shown in Fig. 6d. This result indicates that the as-synthesized black peony-like BiOCl sample is sufficiently stable in the air and water environments. In addition, phenol degradation experiments were also carried out, it point out that phenol can only be degraded by irradiation black BiOCl in the dark, as shown in Fig. S5–S8.†

For evaluation of the potential full-time photocatalytic applications, Fig. 7 shows the decomposition curves of the RhB dye by the white (blue line) and black (red line) peony-like BiOCl samples recorded with sunlight simulator (AM 1.5G). The original UV/Vis spectra of the RhB solutions at different times are given in Fig. S9.† Because the white BiOCl sample is not able to decompose the RhB at night and response to the sunlight, the white BiOCl can only degrade 20% RhB dye even after 3 days. However, the RhB dye can be completely degraded using the black peony-like BiOCl sample in 3 days, due to the PersP effect and good spectral response to sunlight as shown in Fig. 7. It is important noted that the much longer test time (3 days) should be attributed to the much lower power of the sunlight simulator (20 W) than that of xenon lamp (500 W). This result indicates that the black peony-like BiOCl sample shows the potential prospect of the full-time photocatalytic applications.

According to the above results, a possible PersP mechanism of the black peony-like BiOCl material has been proposed in Fig. 8. (1) At first, the electrons ( $e^-$ ) and holes ( $h^+$ ) are promoted under light irradiation. The electrons are excited up into the  $V_o^{\bullet\bullet}$  levels and then are promoted into CBM under the sunlight irradiation. Subsequently, just like many conventional photocatalysts, a reaction between the electrons in conduction band with an oxidant ( $O_2$ ) would produce a reduced product, and also a reaction between the holes in valence band with a reductant ( $H_2O$ ) would produce an oxidized product. Ultimately, the highly oxidative free hydroxyl radicals ( $\cdot OH$ ) are generated in both the reactions, and the secondary oxidation–reduction reactions take place at the surface of photocatalyst. (2) Just like the batteries, some of the photo-induced electrons can be stored

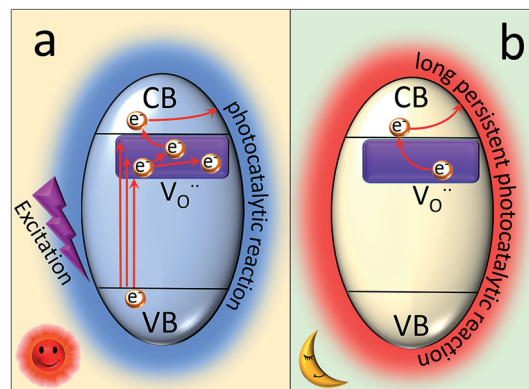


Fig. 8 The PersP mechanism of the black peony-like BiOCl material.

in the levels of  $V_o^{\bullet\bullet}$  acted as traps for an approximately long time. (3) When night is coming, the stored electrons in traps can be thermally released into the CBM *via* the thermal excitation at room temperature. These electrons can also react with oxidant ( $O_2$ ) and produce reduced product the highly oxidative free hydroxyl radicals ( $\cdot OH$ ). As a consequence, it can carry out the oxidation–reduction reactions to degrade the organic pollutions even lack of light irradiation, *i.e.*, PersP effect.

## Conclusions

The black peony-like BiOCl material is able to continuously degrade RhB dye after removing visible irradiation light just like the persistent luminescence. Accordingly, a new concept is defined for the first time: “Persistent Photocatalysis (PersP)” effect. The results of the RhB decomposition experiments demonstrate the PersP effect. It reveals that the PersP effect is highly related to the thermal release of the carriers in the traps ( $V_o^{\bullet\bullet}$ ). Due to the newly discovered PersP effect, the black peony-like BiOCl material shows the potential prospect of the full-time photocatalytic applications. Based on the results, a possible PersP mechanism of the black peony-like BiOCl material has been proposed.

## Acknowledgements

This work was supported by the National Nature Science Foundation of China (No. 10904057, 51202099, 61376011), National Natural Science Foundation of China (51402139), the Fundamental Research Funds for the Central Universities (Lzujbky-2016-129), and the Fundamental Research Funds for Central Universities (No. Lzujbky-2015-112), and the National Science Foundation for Fostering Talents in Basic Research of the National Natural Science Foundation of China (No. 041105 and 041106).

## References

- 1 F. Han, V. S. R. Kambala, M. Srinivasan, D. Rajarathnam and R. Naidu, *Appl. Catal., A*, 2009, **359**, 25–40.
- 2 S. Malato, P. Fernández-Ibáñez, M. I. Maldonado, J. Blanco and W. Gernjak, *Catal. Today*, 2009, **147**, 1–59.

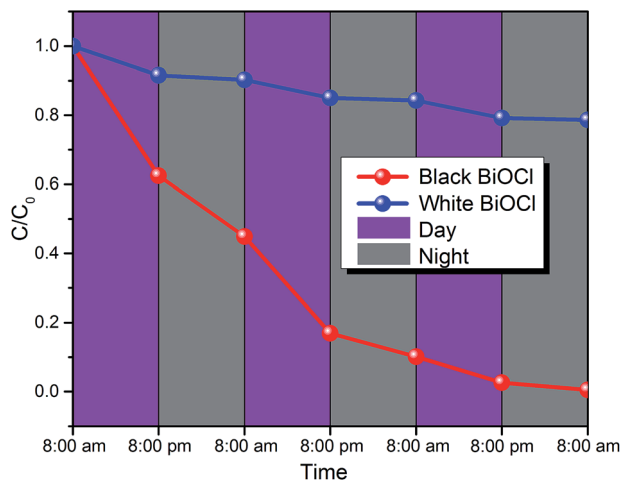


Fig. 7 The potential full-time photocatalytic applications.



- 3 L. Ye, X. Jin, Y. Leng, Y. Su, H. Xie and C. Liu, *J. Power Sources*, 2015, **293**, 409–415.
- 4 Q. Wang, J. Hui, Y. Huang, Y. Ding, Y. Cai, S. Yin, Z. Li and B. Su, *Mater. Sci. Semicond. Process.*, 2014, **17**, 87–93.
- 5 K. Chen, J. Li, W. Wang, Y. Zhang, X. Wang and H. Su, *Mater. Sci. Semicond. Process.*, 2012, **15**, 20–26.
- 6 Z. Jia, D. Ren, L. Xu and R. Zhu, *Mater. Sci. Semicond. Process.*, 2012, **15**, 270–276.
- 7 K. Sayama, H. Hayashi, T. Arai, M. Yanagida, T. Gunji and H. Sugihara, *Appl. Catal., B*, 2010, **94**, 150–157.
- 8 I. Tsuji, H. Kato and A. Kudo, *Chem. Mater.*, 2006, **18**, 1969–1975.
- 9 S. Peng, Y. Huang and Y. Li, *Mater. Sci. Semicond. Process.*, 2013, **16**, 62–69.
- 10 A. Ishikawa, T. Takata, T. Matsumura, J. N. Kondo, M. Hara, H. Kobayashi and K. Domen, *J. Phys. Chem. B*, 2004, **108**, 2637–3642.
- 11 J. Sato, N. Saito, Y. Yamada, K. Maeda, T. Takata, J. N. Kondo, M. Hara, H. Kobayash, K. Domen and Y. Inoue, *J. Am. Chem. Soc.*, 2005, **127**, 4150–4151.
- 12 K. Maeda, K. Teramura, D. Lu, T. Takata, N. Saito, Y. Inoue and K. Domen, *Nature*, 2006, **440**, 295.
- 13 H. Li, S. Yin, Y. Wang and T. Sato, *J. Catal.*, 2012, **286**, 273–278.
- 14 X. Ma, J. Zhang, H. Li, B. Duan, L. Guo, M. Que and Y. Wang, *J. Alloys Compd.*, 2013, **580**, 564–569.
- 15 Y. Mei, H. Xu, J. Zhang, Z. Ci, M. Duan, S. Peng, Z. Zhang, W. Tian, Y. Lu and Y. Wang, *J. Alloys Compd.*, 2015, **622**, 908–912.
- 16 P. Feng, Y. Wei, Y. Wang, J. Zhang, H. Li, Z. Ci and R. J. Xie, *J. Am. Ceram. Soc.*, 2016, **99**, 2368–2375.
- 17 F. Clabau, X. Rocquefelte, S. Jobic, P. Deniard, M.-H. Whangbo, A. Garcia and T. L. Mercier, *Chem. Mater.*, 2005, **17**, 3904–3912.
- 18 B. Liu, Z. Qi, M. Gu, X. Liu, S. Huang and C. Ni, *J. Phys.: Condens. Matter*, 2007, **19**, 436215.
- 19 N. Suriyamurthy and B. S. Panigrahi, *J. Lumin.*, 2008, **128**, 1809–1814.
- 20 X. Xu, Y. Wang, Y. Gong, W. Zeng and Y. Li, *Opt. Express*, 2010, **18**, 16989–16994.
- 21 Y. Jin, Y. Hu, L. Chen, X. Wang and A. Setlur, *J. Am. Ceram. Soc.*, 2014, **97**, 2573–2579.
- 22 J. Zhang, R. Hu, Q. Qin, D. Wang, B. Liu, Y. Wen, M. Zhou and Y. Wang, *J. Lumin.*, 2012, **132**, 2590–2594.
- 23 Y. Li, C. Li, X. Sun, Z. Zhang, Z. Peng, J. Zhang and J. Zhao, *Mater. Lett.*, 2014, **116**, 98–100.
- 24 T. Ihara, *Appl. Catal., B*, 2003, **42**, 403–409.
- 25 L. Ye, K. Deng, F. Xu, L. Tian, T. Peng and L. Zan, *Phys. Chem. Chem. Phys.*, 2012, **14**, 82–85.
- 26 J. Jiang, L. Zhang, H. Li, W. He and J. J. Yin, *Nanoscale*, 2013, **5**, 10573–10581.
- 27 G. Li, B. Jiang, S. Xiao, Z. Lian, D. Zhang, J. C. Yu and H. Li, *Environ. Sci.: Processes Impacts*, 2014, **16**, 1975–1980.
- 28 L. Li, Y.-h. Wang, H. Li, H.-j. Huang and H. Zhao, *RSC Adv.*, 2015, **5**, 57193–57200.
- 29 G. Zhu, M. Hojamberdiev, C. Tan, L. Jin, C. Xu, Y. Liu, P. Liu and J. Zhou, *Mater. Chem. Phys.*, 2014, **147**, 1146–1156.
- 30 J. Jiang, K. Zhao, X. Xiao and L. Zhang, *J. Am. Chem. Soc.*, 2012, **134**, 4473–4476.
- 31 B. Qu, B. Zhang, L. Wang, R. Zhou and X. C. Zeng, *Chem. Mater.*, 2015, **27**, 2195–2202.
- 32 Y. Cong, B. Li, S. Yue and D. Fan, *J. Phys. Chem. C*, 2009, **113**, 13974–13978.
- 33 X. Xu, Y. Wang, Y. Gong, W. Zeng and Y. Li, *Opt. Express*, 2010, **18**, 16989–16994.

